

A clustering method for misaligned curves

Yu-Hsiang Cheng

e-mail: 96354501@nccu.edu.tw

and

Tzee-Ming Huang*

e-mail: tmhuang@nccu.edu.tw

and

Su-Fen Yang

e-mail: yang@mail2.nccu.tw

1. Introduction

Functional data are often observed over time and it is usual that a set of data curves show a common pattern with some variation in time. Before performing further analyses on data curves, such as estimating the common pattern, synchronizing the observed curves is necessary. Thus, curve alignment is an important problem in functional data analysis.

In the literature, many curve alignment methods have been proposed. One approach for curve alignment is landmark registration in [Kneip and Gasser \(1992\)](#). Landmarks are selected characteristics of curves, such as peaks or valleys. Another approach for curve alignment is continuous monotone registration, in which smooth monotone time transformations or warping functions are used to align individual curves to target curves. Curve alignment methods based on continuous monotone registration can be found in [Silverman \(1995\)](#), [Ramsay and Li \(1998\)](#), [Kneip et al. \(2000\)](#), [Gervini and Gasser \(2004\)](#), and [Telesca and Inoue \(2008\)](#). [James James \(2007\)](#) proposed a curve alignment method based on moments, which is a hybrid of the landmark approach and the continuous monotone registration approach.

In the past few years, some authors have investigated the clustering problem for misaligned curves. [Tang and Müller \(2009\)](#) proposed a two-step clustering method. In the first step, curves are aligned using estimated cluster-specific warping functions. In the second step, the aligned curves can be clustered using any existing clustering method, such as k -means clustering or hierarchical clustering. In this method, it is assumed that the warping functions are non-linear and satisfy the boundary condition. [Liu and Yang \(2009\)](#) proposed the SACK

*Corresponding author.

model and provided an estimation procedure using the EM algorithm. Later, Sangalli et al. (2010) proposed a k -means algorithm for clustering misaligned curves. In contrast to the approach in Tang and Müller (2009), in both Liu and Yang (2009) and Sangalli et al. (2010), linear warping functions are considered, and curve alignment and clustering are performed simultaneously, as summarized in Table 1.

TABLE 1
Comparison between our method and other clustering methods

	k-means	SACK	Two-step clustering	Our method
Simultaneous clustering and alignment	Yes	Yes	No	Yes
Linear warping function	Yes	Yes	No	No

In our option, it is better to perform alignment and clustering simultaneously. For instance, when we use the two-step clustering in Tang and Müller (2009), not all curves in the same cluster can be aligned well, as shown in Figure 5. It seems more efficient to perform alignment and clustering simultaneously. For using linear warping functions or nonlinear warping functions, we do not prefer one to the other and a suitable choice should be made based on the nature of data.

In this paper, we provide a method for clustering misaligned curves under the same assumptions for warping functions as in Tang and Müller (2009). For the proposed method, we include a parameter λ_0 to adjust the penalty for large time variation. If it is desirable to put curves with different degrees of time variation into different groups, this can be done using a large λ_0 . We organize this paper as follows. In Section 2, the details of this proposed method and theoretical result are given. Some results of simulation studies and analyses for two real data sets are presented in Sections 3 and 4. Discussion and suggestions are given in Section 5. Proofs are given in Section 6.

2. Methodology

In this section, we will first describe the set-up of the clustering problem and introduce the similarity measure in Section 2.1. Next, we give an overview of the proposed clustering process in Section 2.2. A theoretical result for curve updating is given in Section 2.3.

2.1. Similarity measure

We consider the problem of clustering m_0 data curves y_1, \dots, y_{m_0} , where the curves are observed at time points $0 = t_1 < t_2 \dots < t_n = 1$. For $i = 1, \dots, m_0$

and $j = 1, \dots, n$, let $y_i(t_j)$ denote the observed value of curve y_i at time point t_j . We assume that these curves can be modelled as

$$y_i(t_j) = f_{0,i}(t_j) + \varepsilon_{ij},$$

where $f_{0,i}$ is called the shape function of curve y_i and ε_{ij} s are independent errors with mean zero. The goal of clustering is to assign curves into groups so that similar curves are in the same group, and the curve similarity measure will be introduced in this section.

For two curves with shape functions f_0 and g_0 that do not need to be aligned, a usual similarity measure is

$$r(f_0, g_0) = \frac{\langle f_0, g_0 \rangle}{\|f_0\| \|g_0\|},$$

where

$$\langle f_0, g_0 \rangle = \int_0^1 (f_0(x) - Ef_0)(g_0(x) - Eg_0) dx,$$

$Ef_0 = \int_0^1 f_0(x) dx$, $Eg_0 = \int_0^1 g_0(x) dx$, $\|f_0\| = \sqrt{\langle f_0, f_0 \rangle}$ and $\|g_0\| = \sqrt{\langle g_0, g_0 \rangle}$. Note that $r(f_0, g_0) \leq 1$ and $r(f_0, g_0) = 1$ means that the two curves with shape functions f_0 and g_0 have the same shape (up to a scale and level change).

Our curve similarity measure is based on the similarity measure r for the warped curves, and we consider warping functions in the space

$$\mathcal{M} = \{\psi : \psi \in \mathcal{M}_0 : \psi(0) = 0, \psi(1) = 1 \text{ and } \psi^{-1} \in \mathcal{M}_0\},$$

where \mathcal{M}_0 is the space of continuously differentiable increasing functions defined on $[0, 1]$. The boundary constraint $\psi(0) = 0$ and $\psi(1) = 1$ can also be found in [Ramsay and Silverman \(1997\)](#) and is called the common endpoints condition in [Tang and Müller \(2009\)](#). Note that warping functions satisfying the boundary constraint cannot be linear unless they are equal to the identity function, and as such, we consider nonlinear warping functions.

Below we will define our curve similarity measure. For two curves with shape functions f and g , and for ψ in \mathcal{M} , define

$$\rho^*(f, g|\psi) = r(f, g \circ \psi) - \lambda_0 \left(\int_0^1 \left(\frac{d}{dt} \psi(t) - 1 \right)^2 dt \right) \quad (1)$$

and $\rho(f, g|\psi) = \left(\rho^*(f, g|\psi) + \rho^*(g, f|\psi^{-1}) \right) / 2$, where λ_0 is a non-negative parameter. Then, the similarity measure between f and g is defined as

$$\rho(f, g) = \max_{\psi \in \mathcal{M}} \rho(f, g|\psi).$$

Let $\psi_0 = \arg \max_{\psi \in \mathcal{M}} \rho(f, g|\psi)$, then we use ψ_0 as the warping function when aligning f to g and use ψ_0^{-1} as the warping function when aligning g to f .

Note that our similarity measure depends the parameter λ_0 in (1). λ_0 controls the degree of time variation. For a warping function $\psi \in \mathcal{M}$, the integral

$\int_0^1 \left(\frac{d}{dt} \psi(t) - 1 \right)^2 dt = 0$ implies that ψ is the identity function. Using a large λ_0 thus gives a large penalty for using warping functions that deviate from the identity function, and thus when the curves are clustered, the resulting time variation within the same group is expected to be limited. A similar penalty term for the warping function can be found in Section 5.4.2 in [Ramsay and Silverman \(1997\)](#). Some authors argue that in curve clustering, curve alignment is not always necessary if one would like to consider time variation as a clustering factor ([Jacques and Preda \(2014\)](#)). In that case, one can use a large λ_0 in our similarity measure.

For convenience in evaluating the similarity measure, all data curves and warping functions are approximated using splines. We treat the approximate data curves as curves without errors and will not distinguish between the shape function of a data curve and the data curve itself hereafter.

2.2. Clustering method

In our clustering method, curves are updated so that curves that are similar enough become more similar and then eventually can be combined to form clusters. In the problem of clustering points, the idea of updating points can be found in [Fukunaga and Hostetler \(1975\)](#), [Chen and Shiu \(2007\)](#), and [Shiu and Chen \(2012\)](#). Chen and Shiu (2007, 2012) proposed a self-updating algorithm where points are moved toward their neighbors to form clusters automatically. Our approach is similar to Chen and Shiu's approach since in both our method and Chen and Shiu's algorithm, curves (or points) are updated using weighted averages. However, the weighting schemes are different. Our weighting scheme is based on Theorem 1 in Section 2.3.

To implement our clustering method, we need to choose a set of curve combination thresholds S_c and a clustering index such as the Silhouette coefficient in [Rousseeuw \(1987\)](#). When S_c contains several threshold values, we obtain the clustering result for each threshold value and then determine the final clustering result based on the clustering index. For most of our simulation studies, S_c consists of 4 points near the 75% quantile of similarity measures of original curves excluding one's. Below we describe our clustering method when S_c has only one threshold value c^* . First, we start an iterative process, where in each iteration, we perform

- (A) curve combination and
- (B) curve updating.

For curve combination, two curves can be combined if their similarity measure exceeds the given threshold c^* . After curves are combined, curves will be updated. The iterative process stops when the average curve similarity measure remains stable. Note that at the end of this iterative process, it is possible that all curves are combined into one curve. To obtain a final clustering result from the whole iterative process, in each iteration, if some curves are combined in

Step (A), then we obtain a candidate clustering result based on the updated curves after Step (A) and before Step (B) in that iteration. Thus at the end of the iterative process, several candidate clustering results are obtained, and the candidate result with the best clustering index is chosen as the final clustering result, where the clustering indexes are calculated based on the similarity measures of the original curves. The clustering procedure for a given combination threshold c^* is given in Figure 1. Details for (B) curve updating, (A) curve combination and (C) obtaining a candidate clustering result in each iteration are given in Sections 2.2.1, 2.2.2 and 2.2.3 respectively.

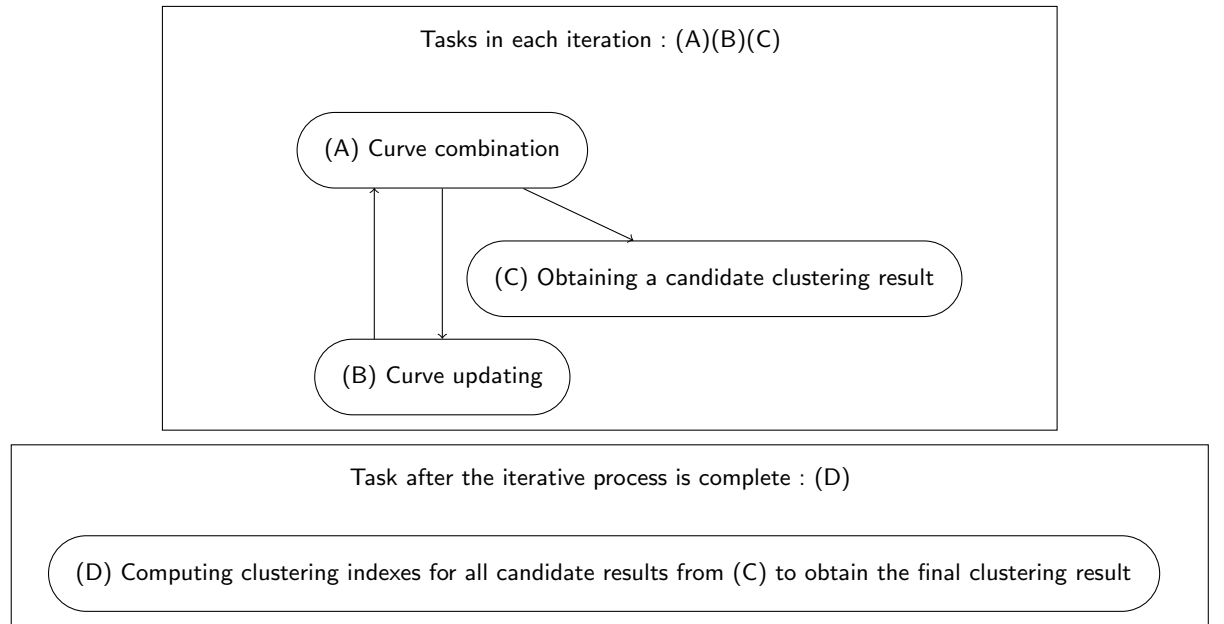


FIG 1. Diagram of the clustering procedure for a given combination threshold c^*

2.2.1. Curve updating

In the curve updating step, suppose that we have several curves to be updated. Then curves are updated one at a time, and before each curve is updated, all curves are normalized so that their L^2 norms are equal to one. Let f_1 denote the curve to be updated and f_2, \dots, f_k denote the rest curves. Then we update f_1 to

$$f_1^* = \left(\frac{\lambda}{\lambda + 1} \right) f_1 + \left(\frac{1}{\lambda + 1} \right) \sum_{j=2}^k \theta_j \frac{f_j \circ \psi_j}{\|f_j \circ \psi_j\|},$$

where $\lambda > 0$, $\theta_j \in [0, 1]$ for $j \geq 2$, $\sum_{j=2}^k \theta_j = 1$, and for $2 \leq j \leq k$, ψ_j is the warping function in \mathcal{M} when aligning f_1 to f_j .

To describe θ_j s, we introduce some notations. For $2 \leq j \leq k$, define $E_j f = \int_0^1 f(t) \frac{d}{dt} \psi_j(t) dt$ for a real value function f on $[0, 1]$. For two real valued functions f and g on $[0, 1]$, define

$$\langle f, g \rangle_j = E_j(f - E_j f)(g - E_j g)$$

and $\|f\|_j = \sqrt{\langle f, f \rangle_j}$. Then for $2 \leq j \leq k$, we set $\theta_j = 0$ if

$$\langle f_1, f_j \circ \psi_j \rangle \leq 0,$$

$$\left\langle \frac{f_j \circ \psi_j}{\|f_j \circ \psi_j\|}, \sum_{\ell=2}^k \frac{f_\ell \circ \psi_\ell - \langle f_\ell \circ \psi_\ell, f_1 \rangle f_1}{\|f_\ell \circ \psi_\ell\|} \right\rangle \leq 0, \quad (2)$$

or

$$\sum_{\ell=2}^k \left\langle \frac{f_j \circ \psi_j}{\|f_j \circ \psi_j\|}, \frac{1}{\|f_1\|_\ell} \left(f_\ell \circ \psi_\ell - \frac{\langle f_\ell \circ \psi_\ell, f_1 \rangle_\ell f_1}{\|f_1\|_\ell^2} \right) \right\rangle_\ell \leq 0. \quad (3)$$

For the θ_j s that are nonzero, we choose θ_j s to be proportional to $n_j w_{1,j}^\tau$, where n_j is the number of original curves that are updated/combined to form the curve f_j ,

$$w_{1,j} = \frac{\rho(f_1, f_j)}{\max\{\rho(f_1, f_j) : \theta_j > 0\}},$$

$\tau = \log(0.5)/\log(\text{Ind}_{\max})$ and Ind_{\max} is the maximum of the similarity measures that are less than 1 for the original data curves.

λ is computed based on the θ_j s. To obtain λ , let

$$g_0 = \sum_{j=2}^k \theta_j \frac{f_j \circ \psi_j}{\|f_j \circ \psi_j\|}, \quad s = \sum_{j=2}^k \frac{f_j \circ \psi_j}{\|f_j \circ \psi_j\|},$$

$$s_0 = \sum_{j=2}^k \frac{f_j \circ \psi_j - \langle f_j \circ \psi_j, f_1 \rangle f_1}{\|f_j \circ \psi_j\|},$$

then λ is the maximum of the following two quantities *LC5* and *LC6*:

$$LC5 = \frac{\|g_0 - \langle g_0, f_1 \rangle f_1\|^2 \langle s, f_1 \rangle^2 - \langle g_0, s_0 \rangle^2}{2 \langle s, f_1 \rangle \langle g_0, s_0 \rangle} - \langle g_0, f_1 \rangle \quad (4)$$

and

$$LC6 = \max \left(\frac{\sum_{j=2}^k \beta_j}{\sum_{j=2}^k \alpha_j}, \max_{2 \leq j \leq k} \max (E_j, |B_j|) \right), \quad (5)$$

where

$$\beta_j = \frac{1}{2} (A_j E_j^2 + B_j D_j + |B_j| E_j) + \frac{3}{\sqrt{2}} (|A_j| + 1) (|D_j| + E_j)^2,$$

$$A_j = \frac{\langle f_1, f_j \circ \psi_j \rangle_j}{\|f_1\|_j}, \quad B_j = \frac{\langle g_0, f_j \circ \psi_j \rangle_j}{\|f_1\|_j}, \quad D_j = \frac{2 \langle f_1, g_0 \rangle_j}{\|f_1\|_j^2},$$

$$E_j = \frac{\|g_0\|_j}{\|f_1\|_j}, \text{ and } \alpha_j = B_j - \frac{1}{2} A_j D_j.$$

2.2.2. Details for curve combination

We briefly state the tasks in the step of curve combination. In this step, we first put sets of similar curves into clusters, then for each cluster, align curves in the cluster to a reference curve, combine the aligned curves in the cluster to form a representative curve, and replace the curves in the cluster by the cluster representative. The representative curve is the fitted B-spline curve to the aligned data curves using weighted least square regression, where the reference curve for alignment is chosen as the curve in the cluster with the largest average of similarity measures to other curves in the cluster, and the weight for each curve in the weighted least square regression is the number of original curves that are updated/combined to form this curve. Here two curves are considered similar if their similarity measure exceeding c^* .

The main difficulty in the step of curve combination is that sometimes we have a conflictive situation in clustering. For instance, suppose that we have a curve f_1 that is similar to two curves f_2 and f_3 , but f_2 and f_3 are not similar, then it is not clear how these three curves should be combined. In such case, we make use of the clustering index to help resolve this difficulty. Here the clustering index is computed based on the updated curves, not the original curves. For a combination result that assigns several updated curves to p groups G_1, \dots, G_p for combination, let $\nu(G_1, \dots, G_p)$ denote the clustering index based on the updated curves.

Below we give the steps for assigning m curves f_1, \dots, f_m into clusters for combination.

1. Compute

$$\rho(f_i) = \sum_{j=1, \dots, m, \rho(f_i, f_j) > c^*} \rho(f_i, f_j),$$

for $1 \leq i \leq m$.

2. Sort the m functions f_1, \dots, f_m by $\rho(f_i)$ s (from largest to smallest). Let S be the sequence of sorted functions.
3. Let f^* be the first function in S . Form a new group G_0 including f^* by carrying out the steps (a)–(c) below and then remove the curves in G_0 from S .
 - (a) Collect the functions f_i s in S that satisfy $\rho(f^*, f_i) > c^*$, and then sort these functions by $\rho(f^*, f_i)$ s (from largest to smallest). Let P be the sequence of the above sorted functions.
 - (b) Let $G_0 = \{f^*\}$, and then add the functions in P to G_0 in turn under the constraint that each newly added function is similar to all functions in G_0 .
 - (c) For every function in G_0 , check whether it has similar function(s) outside G_0 .
 - If it has no similar function outside G_0 , then G_0 is the new group containing f^* .

- If it has similar function(s) outside G_0 , carry out (**) to update G_0 . The resulting G_0 is the new group containing f^* .

(**) For all functions in G_0 , determine in turn whether they will stay in G_0 according to the following criterion: for a function f_0^* in G_0 , let $s(f_0^*)$ be the collection of similar curves of f_0^* and $s(G_0)$ be the collection of curves that are similar to all curves in G_0 . Let $D = s(f_0^*) \cap s(G_0)^c$, where $s(G_0)^c$ is the complement of set $s(G_0)$. f_0^* will stay in G_0 if either of the following two conditions are satisfied:

- (1) D is an empty set;
- (2) $\nu(G_0 \cup \{f_0^*\}, \{s^*\}) > \nu(\{f_0^*, s^*\}, G_0)$, where s^* is the most similar curve to f_0^* among the curves in D .

4. Repeat 3 until S is empty.

Following the above steps, we can assign f_1, \dots, f_m into clusters and then combine curves in the same cluster.

2.2.3. Obtaining a candidate clustering result

In this section, we give details for obtaining a candidate clustering result (Step (C) in Figure 1). Note that in the curve combination step, we put some curves in clusters for combination and leave other curves outside those clusters, so we only have a partial clustering result. For curves that are not assigned into clusters for combination, we treat those curves as unassigned curves and then perform further clustering to obtain a complete clustering result as a candidate clustering result. The details are given below.

Let \mathcal{G}_0 and S_0 be the collections of groups and unassigned curves respectively based on the partial clustering result in curve combination. Let p_0 be the number of groups in \mathcal{G}_0 and q_0 be the number of unassigned curves in S_0 . Also, for a clustering result that assigns several updated curves to p groups G_1, \dots, G_p , let $\nu_0(G_1, \dots, G_p)$ denote the similarity measure for the clustering result computed based on the original curves. Then we can obtain the candidate clustering result by carrying out the following steps for the case $p_0 \geq 2$ and $q_0 \geq 1$.

1. Set $\mathcal{G} = \mathcal{G}_0$ and $S = S_0$.
2. Suppose that \mathcal{G} is the collection of p groups G_1, \dots, G_p , and S is nonempty. For every curve g in S , compute $\nu_0(G_1 \cup \{g\}, \dots, G_p)$, \dots , $\nu_0(G_1, \dots, G_p \cup \{g\})$ and $\nu_0(G_1, \dots, G_p, \{g\})$. If the clustering result that includes $G_k \cup \{g\}$ has the largest ν_0 value for some $k \in \{1, \dots, p\}$, then adds g to group G_k and removes it from S .
3. Suppose that after Step 2, S remains nonempty and $S = \{h_1, \dots, h_q\}$ and \mathcal{G} becomes the collection of p groups G_1^*, \dots, G_p^* . For $i = 1, \dots, q$, compute $\nu_0(G_1^*, \dots, G_p^*, \{h_i\})$ and let h^* be the h_i with the largest $\nu_0(G_1^*, \dots, G_p^*, \{h_i\})$. Add the singleton $\{h^*\}$ to \mathcal{G} so that \mathcal{G} includes exactly $(p + 1)$ groups: $G_1^*, \dots, G_p^*, \{h^*\}$. Remove h^* from S .
4. Repeat the steps 2 and 3 until S is empty.

5. A complete clustering result is given by \mathcal{G} .

The above steps for obtaining a complete clustering result \mathcal{G} based on a partial clustering result characterized by a collection of non-singleton groups \mathcal{G}_0 and a collection of unassigned curves S_0 can be viewed as a function of \mathcal{G}_0 and S_0 . We will name this function *cluster.1* and denote the function output by *cluster.1*(\mathcal{G}_0, S_0) based on input \mathcal{G}_0 and S_0 . This function will be also used to handle the cases other than $p_0 \geq 2$ and $q_0 \geq 1$.

For cases other than $p_0 \geq 2$ and $q_0 \geq 1$, the details for obtaining a candidate clustering result \mathcal{G} based on the partial clustering result from curve combination are given below.

- $p_0 = 0$ and $q_0 = 2$. Let g_1 and g_2 be the two curves in S_0 . If the two curves g_1 and g_2 are similar, then let \mathcal{G} be the clustering result including only one group $\{g_1, g_2\}$. Otherwise, let \mathcal{G} be the clustering result of two singletons $\{g_1\}$ and $\{g_2\}$.
- $p_0 = 0$ and $q_0 \geq 3$. Suppose that $S_0 = \{g_i : i = 1, \dots, q_0\}$.
 - (1) For $i = 1, \dots, q_0$, compute $\rho(g_i) = \sum_{j=1}^{q_0} \rho(g_i, g_j)$. Let g_1^* be the curve g_i with the largest $\rho(g_i)$ and form a new group $\{g_1^*\}$.
 - (2) Compute $\nu_0(\{g_1^*\}, \{g_i\})$ for $g_i \neq g_1^*$, let g_2^* be the curve g_i with the largest $\nu_0(\{g_1^*\}, \{g_i\})$ for $g_i \neq g_1^*$. Form the second group $\{g_2^*\}$.
 - (3) Let $\mathcal{G} = \text{cluster.1}(\{\{g_1^*\}, \{g_2^*\}\}, \{g_i, g_i \neq g_1^*, g_2^*\})$.
- $p_0 = 1$ and $q_0 = 1$. Let G_1 be the only group in the collection \mathcal{G}_0 and g_1 be the only curve in S_0 . Suppose that G_1 is composed of m^* curves f_1, \dots, f_{m^*} . Compute $\kappa_0 = \nu_0(G_1, \{g_1\})$ and $\kappa_i = \nu_0(\{g_1, f_1, \dots, f_{m^*}\} - \{f_i\}, \{f_i\})$ for $i = 1, \dots, m^*$. If some κ_i is larger than κ_0 , put the curve g_1 into G_1 and let \mathcal{G} be the clustering result including exactly the group $G_1 \cup \{g_1\}$. Otherwise, let \mathcal{G} be the clustering result including exactly G_1 and the singleton group $\{g_1\}$.

2.3. Curve updating - theoretical result

The weighting scheme in the curve updating step is based on our Theorem 1 in this section. The theorem gives some conditions on the weights when updating a curve f_1 to a weighted average of f_1 and warped versions of other $(k-1)$ curves f_2, \dots, f_k :

$$f_1^* = \left(\frac{\lambda}{\lambda + 1} \right) f_1 + \left(\frac{1}{\lambda + 1} \right) \sum_{j=2}^k \theta_j \frac{f_j \circ \psi_j}{\|f_j \circ \psi_j\|},$$

where $\lambda > 0$, $\theta_j \in [0, 1]$ for $j \geq 2$, $\sum_{j=2}^k \theta_j = 1$, and for $2 \leq j \leq k$, ψ_j is the warping function in \mathcal{M} when aligning f_1 to f_j . When the conditions in Theorem 1 hold, the updated curve f_1^* is more similar to other curves than f_1 on average in the sense that (6) holds.

We follow the definitions of $\langle \cdot, \cdot \rangle_j$ and $\|\cdot\|_j$ in Section 2.2.1 and state Theorem 1 below.

Theorem 1. *Suppose that the following conditions hold:*

- (C1) $\|f_j\| = 1$ for $1 \leq j \leq k$.
(C2) $\langle f_1, f_j \circ \psi_j \rangle \geq 0$ for $2 \leq j \leq k$.
(C3) $\left\langle \sum_{j=2}^k \theta_j \frac{f_j \circ \psi_j}{\|f_j \circ \psi_j\|}, \sum_{\ell=2}^k \frac{f_\ell \circ \psi_\ell - \langle f_\ell \circ \psi_\ell, f_1 \rangle f_1}{\|f_\ell \circ \psi_\ell\|} \right\rangle > 0$.
(C4) $\sum_{\ell=2}^k \left\langle \sum_{j=2}^k \theta_j \frac{f_j \circ \psi_j}{\|f_j \circ \psi_j\|}, \frac{1}{\|f_1\|_\ell} \left(f_\ell \circ \psi_\ell - \frac{\langle f_\ell \circ \psi_\ell, f_1 \rangle_\ell f_1}{\|f_1\|_\ell^2} \right) \right\rangle_\ell > 0$.
(C5) $\lambda \geq LC5$, where $LC5$ is given in (4).
(C6) $\lambda \geq LC6$, where $LC6$ is given in (5).

Then,

$$\sum_{j=2}^k \rho(f_1^*, f_j) \geq \sum_{j=2}^k \rho(f_1, f_j). \quad (6)$$

The proof of Theorem 1 is given in Section 6.

In our curve updating step, curves are normalized so that (C1) holds, only f_j s satisfying (C2) will be used to update f_1 , weights θ_j s are selected so that (C3) and (C4) hold, and λ is chosen so that (C5) and (C6) hold. To specify θ_j s such that (C3) and (C4) hold, note that (C3) and (C4) are of the form $\sum_{j=1}^k \theta_j C_j > 0$ for some known constants C_j s. We simply set $\theta_j = 0$ when $C_j \leq 0$ for each j to ensure that $\sum_{j=1}^k \theta_j C_j > 0$. The requirement $C_j \leq 0$ for (C3) and (C4) corresponds to (2) and (3) respectively. There are certainly other ways for choosing θ_j s such that (C3) and (C4) hold, but we have not yet explored them.

In (2) and (3), $f_\ell \circ \psi_\ell - \langle f_\ell \circ \psi_\ell, f_1 \rangle f_1$ and $f_\ell \circ \psi_\ell - \langle f_\ell \circ \psi_\ell, f_1 \rangle_j f_1$ are residuals of projecting the warped curve $f_\ell \circ \psi_\ell$ to the space spanned by f_1 with respect to the semi-inner products $\langle \cdot, \cdot \rangle$ and $\langle \cdot, \cdot \rangle_j$ respectively. The effect for setting $\theta_j = 0$ if (2) or (3) holds is so that curves that are very dissimilar to the residuals on average can be excluded, so that the updated curve f_1^* can be more similar to the rest of the curves on average.

3. Simulation studies

In this section, we present results of the simulation studies under various settings with S_c (the set of combination thresholds) taken to be the set $\{q_{1-a} - 0.01 + (0.01 \cdot i/3): i = 0, 1, 2, 3\}$, where q_{1-a} denotes the $100(1-a)\%$ sample quantile of the similarity measures of original curves that are less than one.

In Sections 3.1–3.3, we consider different types of warping functions using the Silhouette index as the clustering index and take $q_{1-a} = q_{0.75}$ for S_c . Recall that for a warping function ψ , we assume that ψ is monotone on $[0, 1]$ and satisfies the boundary condition

$$\psi(0) = 0 \text{ and } \psi(1) = 1. \quad (7)$$

In Section 3.1, we consider warping functions satisfying the boundary condition (7) and the focus is on the effect of parameter λ_0 and the unbalance class size. In Section 3.2, we consider warping functions that violate the boundary condition (7) slightly. In Section 3.3, we consider both linear and nonlinear warping functions to compare our method with the k -means clustering method in Sangalli et al. (2010), which is designed for linear warping functions. The clustering results for the two methods are quite different, as expected.

In Section 3.4, we consider different q_{1-a} values and different clustering index settings. The q_{1-a} values considered are $q_{0.95}$, $q_{0.85}$, $q_{0.65}$, $q_{0.55}$ and $q_{0.45}$. For the clustering index, we try the Dunn index (Dunn (1974)) under different inter-cluster distances and intra-cluster distances to compare the results with those based on the Silhouette index.

In our simulation experiments, we use splines to approximation shape curves and warping functions. All data curves are first approximated using cubic splines, and the knots are selected using the method proposed by Zhou and Shen (2001) with one initial knot at 0.5. Then, we evaluate the approximated curves at 500 equally spaced points in $[0, 1]$ to obtain the approximate observed curves and then perform shape curve approximation. For shape curve approximation, we use cubic splines with 16 equally spaced inner knots, and evaluate shape curves at 500 time points for finding fitted splines using the method of least squares. The shape curve approximation is also performed whenever a new shape curve is obtained during curve updating. For the approximation of warping functions, we use quadratic splines with three equally spaced inner knots. We also use quadratic splines with 23 equally spaced inner knots to approximate the inverse of warping functions.

3.1. Case of warping functions satisfying the boundary condition

We generate three sets of curves G_1 – G_3 . For $i \in \{1, 2, 3\}$, the i -th set is composed of N_i similar curves, which have a common shape function f_i if properly warped. The shape functions for G_1 – G_3 are given below:

$$f_1(t) = \sin(2.5\pi t),$$

$$f_2(t) = (-t^2 + \sin(2\pi t) + 0.25)/1.3,$$

and

$$f_3(t) = \sin(2.5\pi t^{2.5}),$$

for $t \in [0, 1]$. For the warping functions, we consider functions of the form t^α , where $\alpha \in \{0.86 + 0.03(k-1) : k = 1, \dots, 10\}$ so that the boundary condition holds. N_i is either 10 or 20 in this study. For $N_i = 10$, we use warping functions ψ_1, \dots, ψ_{10} , where $\psi_k(t) = t^{0.86+0.03(k-1)}$ for $t \in [0, 1]$ and $k = 1, \dots, 10$. For $N_i = 20$, we use warping functions $\psi_1, \dots, \psi_{10}, \psi_{11}, \dots, \psi_{20}$. Every curve is generated with equally spaced time points $t_1 = 0, \dots, t_{100} = 1$, and the j -th generated curve in the i -th group is

$$y_{ij}(t) = f_i(\psi_j(t)) + \varepsilon_{ij}(t), \quad (8)$$

where $\varepsilon_{ij}(t_1), \dots, \varepsilon_{ij}(t_{100})$ are IID $N(0, \sigma^2)$. Here, $\sigma = 0.15$ or 0.45 .

Note that $f_3(t) = f_1(t^{2.5})$, and thus if G_1 and G_3 curves are properly warped, they will have the same shape function. Figure 2 shows the three sets of curves without errors. It appears that curves in the same group follow a similar pattern since the time variation within each group is not very large. In contrast, for G_1 and G_3 curves, although they have the same shape function when properly warped, the unwarped curves for the two groups show quite different patterns due to large variation in time.

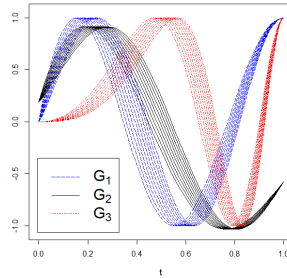


FIG 2. G_1 – G_3 curves without errors

To investigate the effect of λ_0 and class size, two values for λ_0 and seven class sizes are considered, and the adjusted Rand indexes proposed by [Hubert and Arabie \(1985\)](#) for evaluating clustering results are calculated for the following two cases.

- (a) There are two clusters $G_1 \cup G_3$ and G_2 . This clustering case is denoted by $((G_1, G_3), G_2, 2)$.
- (b) There are three clusters G_1 , G_2 , and G_3 . This clustering case is denoted by $(G_1, G_2, G_3, 3)$.

Table 2 shows the adjusted Rand index averages of 30 experiments for Cases (a) and (b), and the standard deviations are given in parentheses. Note that when $\lambda_0 = 0$, the shape functions for G_3 and G_1 curves are perfectly similar according to our similarity measure, and accordingly, our method usually returns the clustering result $((G_1, G_3), G_2, 2)$ that matches Case (a). When $\lambda = 0.5$, the shape functions for G_3 and G_1 curves are less similar since there is a penalty for using warping functions that are different from identity. As a result, our method often returns the clustering result $(G_1, G_2, G_3, 3)$ matches Case (b). This phenomenon is observed under various combinations of class size and λ_0 for each σ . In addition, the effect of class size is not significant.

TABLE 2
Adjusted Rand index averages for different sizes of groups and λ_0 s

$((G_1, G_3), G_2, 2)$	$\sigma = 0.15$		$\sigma = 0.45$	
	$\lambda_0 = 0.0$	$\lambda_0 = 0.5$	$\lambda_0 = 0.0$	$\lambda_0 = 0.5$
$(N1, N2, N3)$				
(10, 10, 10)	1(0)	0.5538(0)	0.9802(0.1009)	0.5513(0.0098)
(10, 10, 20)	1(0)	0.5185(0)	0.9668(0.1448)	0.5179(0.0035)
(10, 20, 10)	1(0)	0.7417(0)	0.9984(0.0089)	0.7403(0.0076)
(20, 10, 10)	0.9974(0.0141)	0.5172(0.0073)	0.9974(0.0141)	0.5185(0)
(20, 20, 10)	0.9990(0.0057)	0.6755(0)	0.9984(0.0086)	0.6745(0.0056)
(20, 10, 20)	1(0)	0.4096(0)	0.9953(0.0179)	0.4082(0.0056)
(10, 20, 20)	1(0)	0.6755(0)	0.9816(0.0753)	0.6730(0.0081)
$(G_1, G_2, G_3, 3)$				
$(N1, N2, N3)$				
(10, 10, 10)	0.5538(0)	1(0)	0.5586(0.0363)	0.9967(0.0125)
(10, 10, 20)	0.5185(0)	1(0)	0.5138(0.0182)	0.9992(0.0046)
(10, 20, 10)	0.7417(0)	1(0)	0.7399(0.0097)	0.9985(0.0082)
(20, 10, 10)	0.5175(0.0058)	0.9982(0.0098)	0.5175(0.0058)	1(0)
(20, 20, 10)	0.6744(0.0062)	1(0)	0.6748(0.0036)	0.9988(0.0063)
(20, 10, 20)	0.4096(0)	1(0)	0.4090(0.0023)	0.9977(0.0088)
(10, 20, 20)	0.6755(0)	1(0)	0.6772(0.0154)	0.9972(0.0091)

3.2. Case of warping functions slightly violating the boundary condition

In this section, we examine the performance of our method when the boundary condition is violated slightly. We generate data using shape functions f_1 , f_2 , and f_3 in Section 3.1, but the warping functions are of the following forms:

$$\psi_a(t) = a_1 t + a_2, t \in [0, 1]$$

and

$$\psi_b(t) = (1 + b_2 - b_1)t^\alpha + b_1, t \in [0, 1],$$

where a_1, a_2, b_1, b_2 are generated from uniform distributions $U(0.975, 1.025)$, $U(0, 0.05)$, $U(0, 0.05)$, and $U(-0.05, 0.05)$, respectively. The range for α is the same as in Section 3.1. Note that ψ_a is a linear function, which is a common choice for warping functions, and ψ_b is a function such that $\psi_b(0) = b_1$ and $\psi_b(1) = 1 + b_2$. The two types of warping functions do not satisfy the boundary condition if $(a_1, a_2) \neq (1, 0)$ and $(b_1, b_2) \neq (0, 0)$. For this part of simulation studies, we only consider $(N1, N2, N3) = (10, 10, 10)$ and $\sigma = 0.15$. The clustering results are shown in Table 3.

In Table 3, the adjusted Rand index averages for different combinations of warping functions and λ_0 values are given for Cases (a) and (b). Due to the

violation of the boundary condition, the clustering performance here is slightly different from when warping functions satisfy the boundary condition. However, for the effect of λ_0 , the phenomenon observed in Section 3.1 is still present here. That is, our method returns results that match the $((G_1, G_3), G_2, 2)$ case well when $\lambda_0 = 0$, and it returns results that match the $(G_1, G_2, G_3, 3)$ case well when $\lambda_0 = 0.5$.

TABLE 3
Adjusted Rand index averages using warping functions ψ_a and ψ_b

	ψ_a		ψ_b	
	$((G_1, G_3), G_2, 2)$	$(G_1, G_2, G_3, 3)$	$((G_1, G_3), G_2, 2)$	$(G_1, G_2, G_3, 3)$
$\lambda_0 = 0.0$	1(0)	0.5538(0)	0.9828(0.0939)	0.5658(0.0652)
$\lambda_0 = 0.5$	0.5538(0)	1(0)	0.5538(0)	1(0)

3.3. Case of warping assumptions not holding

In this section, we compare the clustering result of our method with that of the k -means clustering method in Sangalli et al. (2010), designed for linear warping functions, under two situations: (1) the warping functions are linear and (2) the warping functions satisfy the boundary condition. For our method, the warping assumption is violated in Case (1). For the k -means method, the warping assumption is violated in Case (2). In what follows, the details of simulation data, clustering results, and some discussions are presented. We use the R package “fdama” to perform the k -means clustering method in Sangalli et al. (2010).

First, we consider Case (1). In this experiment, we generate three groups of simulation curves G_4 – G_6 using random functions f_4 – f_6 given below, which are taken from Sangalli et al. (2010) with the modification that a linear function is used to transform the time range from $[0, 2\pi]$ to $[0, 1]$.

$$f_4(t) = (1 + \varepsilon_1) \sin(\varepsilon_2 + (1 + \varepsilon_3)2\pi t) \\ + (1 + \varepsilon_4) \sin\left(\frac{(\varepsilon_2 + (1 + \varepsilon_3)2\pi t)^2}{2\pi}\right), t \in [0, 1],$$

$$f_5(t) = (2 + \varepsilon_1) \sin(\varepsilon_2 + (1 + \varepsilon_3)2\pi t) \\ + (-1 + \varepsilon_4) \sin\left(\frac{(\varepsilon_2 + (1 + \varepsilon_3)2\pi t)^2}{2\pi}\right), t \in [0, 1],$$

and

$$f_6(t) = (1 + \varepsilon_1) \sin\left(\frac{-1}{3} + \varepsilon_2 + \left(\frac{3}{4} + \varepsilon_3\right)2\pi t\right) \\ + (1 + \varepsilon_4) \sin\left(\frac{1}{2\pi} \left(-\frac{1}{3} + \varepsilon_2 + \left(\frac{3}{4} + \varepsilon_3\right)2\pi t\right)^2\right), t \in [0, 1].$$

For each of G_4 – G_6 , 10 curves are generated using f_4 – f_6 respectively, but the random errors in G_4 are the same as those in G_5 and G_6 . The curves in G_4 and G_6 can be synchronized using linear warping functions. The graph of the data curves are shown in Figure 3(a). For the k -means clustering method, the curves

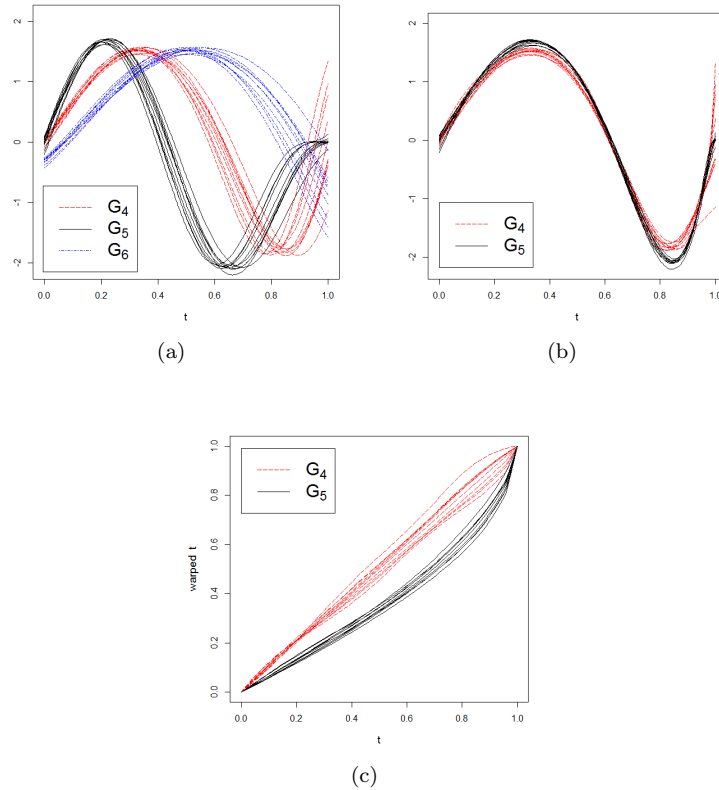


FIG 3. Curves and clustering results for $G_4 - G_6$ using our method

can be clustered into two groups: $G_4 \cup G_6$ and G_5 when the initial centers are specified properly. This result is expected since the curves in G_4 and G_6 can be synchronized by linear warping functions.

For our clustering method with $\lambda_0 = 0.0$, we obtain two groups: $G_4 \cup G_5$ and G_6 . This clustering result is quite different from that of the k -means method, because the curves in G_4 and G_5 have similar patterns when they are aligned using nonlinear warping functions satisfying the boundary condition. Figure 3(c) shows the warping functions when the curves in G_4 and G_5 are aligned to a reference curve and Figure 3 (b) shows the aligned curves. The curves in G_6 cannot be aligned well to the curves in G_4 or G_5 using warping functions satisfying the boundary condition, and as such, they are not clustered into one group under our method.

In the second experiment, we consider Case (2). We use shape functions

$$g_1(t) = \sin(2\pi t^2), t \in [0, 1],$$

$$g_2(t) = \cos(2\pi t^2), t \in [0, 1]$$

and warping functions $\{\varphi_1, \dots, \varphi_4\} = \{t^{0.78}, t^{0.89}, t^{1.11}, t^{1.22}\}$ to generate two groups of simulation curves G_7 and G_8 . Each group is composed of four curves with the same shape function, generated according to (8) but without errors.

In the second experiment, our clustering method with $\lambda_0 = 0.0$, gives the clustering result of two groups G_7 and G_8 . We also apply the k -means clustering method in Sangalli et al. (2010) with the initial number of groups ranging from one to five.

For a given number of clusters k , we use every possible combination of k curves among all data curves as initial cluster centers and obtain the average similarity measures between curves and their cluster centers for the corresponding clustering result. Figure 4 shows the box plot of averages of similarity measures for each $k \in \{1, \dots, 5\}$. This figure shows that the median of averages of similarity measures increases as k increases, and k needs to be at least 3 for the averages of similarity measures to be less sensitive to the choice of initial cluster centers. The result for the k -means method is quite different from that for our method since all the curves in G_7 (or G_8) cannot be aligned well to each other using linear warping functions.

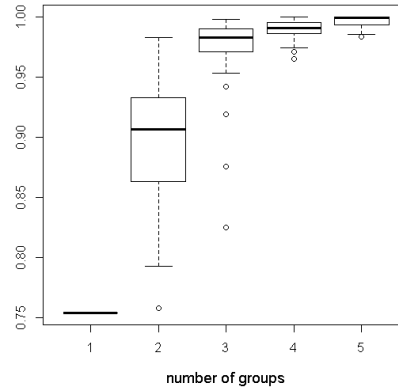


FIG 4. Clustering results for G_7 – G_8 using k -means clustering in Sangalli et al. (2010)

In addition to the above experiments, we also tried the two-stage approach proposed in Tang and Müller (2009). In the first stage, the cluster-specific warping functions were estimated using our similarity measure. In the second stage, we used the function “kmeans.fd” in R package “fda.usc” to perform k -means clustering to the aligned curves. The clustering results were not as good as ours

in terms of the adjusted Rand index averages for the $\lambda_0 = 0$ case. In addition, for the case $\lambda_0 = 0$ and $\sigma = 0.15$, the perfect clustering result is $(G_1 \cup G_3, G_2)$ and our method gives the perfect result in all of the 30 trials. However, the two-stage approach gives the perfect result in only 13 of the 30 trials. Figure 5 shows the warped curves after the first-stage alignment using the two-stage approach. Note that the warped curves in $G_1 \cup G_3$ show larger variation in time as compared to the warped curves in G_2 . As a result, k -means clustering usually assigns the curves in G_2 into the same cluster, but fails to assign the curves in $G_1 \cup G_3$ into the same cluster.

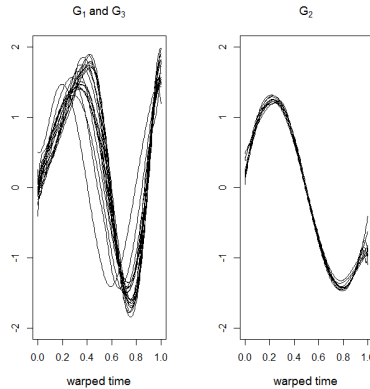


FIG 5. Warped curves after the first-stage alignment

3.4. Effect of q_{1-a} and clustering index

In this section, we investigate the influence of q_{1-a} and clustering index on the proposed clustering method. The simulation data here are the same as those in the case $(N1, N2, N3) = (10, 10, 10)$ in Section 3.1.

First, we apply the proposed method to the simulation data under different q_{1-a} values. Table 4 shows the average Adjusted Rand index corresponding to five q_{1-a} values under $\sigma = 0.15$ and 0.45 . We find that the performance of the proposed method is still satisfactory when $q_{1-a} \in \{q_{45}, q_{55}, q_{65}, q_{85}\}$. When $q_{1-a} = q_{95}$, the proposed method sometimes gives a large number of clusters. This is probably due to the fact that the curves cannot be combined in few iterations and the limit for the number of iterations is set to 10.

Next, we apply the proposed method using the Dunn index to compare the clustering results with those based on the Silhouette index. The Dunn index based on groups G_1, \dots, G_k is defined by

$$\frac{\min_{1 \leq i < j \leq k} d_{inter}(G_i, G_j)}{\max_{1 \leq i \leq k} d_{intra}(G_i)},$$

TABLE 4
Adjusted Rand index averages for different q_{1-a} values and λ_0 s

$((G_1, G_3), G_2, 2)$	$\sigma = 0.15$		$\sigma = 0.45$	
	$\lambda_0 = 0.0$	$\lambda_0 = 0.5$	$\lambda_0 = 0.0$	$\lambda_0 = 0.5$
q_{95}	0.9728(0.1492)	0.5538(0)	0.6606(0.4551)	0.5076(0.1112)
q_{85}	1(0)	0.5538(0)	0.9986(0.0076)	0.5538(0)
q_{65}	1(0)	0.5538(0)	0.9986(0.0076)	0.5538(0)
q_{55}	1(0)	0.5538(0)	0.9986(0.0076)	0.5538(0)
q_{45}	1(0)	0.5538(0)	0.9931(0.0307)	0.5538(0)
$(G_1, G_2, G_3, 3)$	$\sigma = 0.15$		$\sigma = 0.45$	
	$\lambda_0 = 0.0$	$\lambda_0 = 0.5$	$\lambda_0 = 0.0$	$\lambda_0 = 0.5$
q_{95}	0.5493(0.0251)	1(0)	0.4136(0.2027)	0.9303(0.1702)
q_{85}	0.5538(0)	1(0)	0.5523(0.0087)	1(0)
q_{65}	0.5538(0)	1(0)	0.5523(0.0087)	1(0)
q_{55}	0.5538(0)	1(0)	0.5523(0.0087)	1(0)
q_{45}	0.5538(0)	1(0)	0.5519(0.0088)	1(0)

where d_{inter} and d_{intra} are inter-cluster distance and intra-cluster distance respectively. In this simulation study, we use three inter-cluster distances (I1)–(I3) and two intra-cluster distances (J1)–(J2) when evaluating the Dunn index. The definitions of these distances can be found in Soler et al. (2013) and stated below. In the following descriptions, $d(a, b)$ denotes the distance between two elements a and b and $|A|$ denotes the number of elements in group A .

- $d_{inter}(G_i, G_j)$
 - (I1): $\min_{x_1 \in G_i, x_2 \in G_j} d(x_1, x_2)$
 - (I2): $\max_{x_1 \in G_i, x_2 \in G_j} d(x_1, x_2)$
 - (I3): $\frac{1}{|G_i||G_j|} \sum d(x_1, x_2)$, where $x_1 \in G_i$ and $x_2 \in G_j$
- $d_{intra}(G_i)$
 - (J1): $\max_{x_1, x_2 \in G_i, x_1 \neq x_2} d(x_1, x_2)$
 - (J2): $\frac{1}{|G_i|(|G_i|-1)} \sum d(x_1, x_2)$, where $x_1, x_2 \in G_i$ and $x_1 \neq x_2$

In Table 5, we show the adjusted Rand index averages for the proposed method using Dunn index with the inter-cluster distances and intra-cluster distances mentioned above. Only the case $(\sigma, q_{1-a}) = (0.15, q_{75})$ is considered. We find that the Adjusted Rand index averages are similar for the six cases (I1, J1) – (I3, J2), and the clustering results are very similar to the results based on Silhouette index.

TABLE 5
Adjusted Rand index averages based on Dunn index

$((G_1, G_3), G_2, 2)$	$(I1, J1)$	$(I1, J2)$	$(I2, J1)$	$(I2, J2)$	$(I3, J1)$	$(I3, J2)$
$\lambda_0 = 0.0$	1(0)	1(0)	0.9971(0.0159)	1(0)	0.9971(0.0159)	1(0)
$\lambda_0 = 0.5$	0.5538(0)	0.5538(0)	0.5538(0)	0.5538(0)	0.5538(0)	0.5538(0)
$(G_1, G_2, G_3, 3)$	$(I1, J1)$	$(I1, J2)$	$(I1, J3)$	$(I2, J1)$	$(I2, J2)$	$(I2, J3)$
$\lambda_0 = 0.0$	0.5538(0)	0.5538(0)	0.5535(0.0019)	0.5538(0)	0.5535(0.0019)	0.5538(0)
$\lambda_0 = 0.5$	1(0)	1(0)	1(0)	1(0)	1(0)	1(0)

4. Data applications

In this section, we apply our method to two data sets using $q_{1-a} = q_{75}$.

4.1. Berkeley growth study data

The Berkeley growth study data set (Tuddenham and Snyder (1954)) consists of the heights of 39 boys and 54 girls at 31 time points from when they were a year old to when they were 18 years old. Figure 6(a) shows these height curves, and Figure (b) shows the corresponding growth velocity curves that are obtained using the smoothing technique in Section 4.2 in Ramsay and Silverman (1997). In this analysis, we apply the proposed clustering method to the growth velocity curves instead of the original height curves. The height curves are increasing functions of age, and thus they inevitably form similar curves with $\lambda_0 = 0$. For convenience, we apply a linear function to transform the age range $[1, 18]$ into $[0, 1]$. Figure 7 shows the clustering results of these velocity curves from our

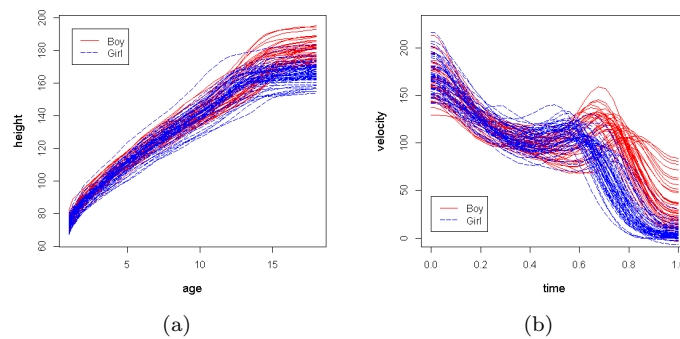


FIG 6. Height and velocity curves for the Berkeley growth study

clustering method with $\lambda_0 = 0.0$ and 0.5 . In both cases, these velocity curves

are classified into two groups. We show the aligned velocity curves in Figures 7(a) and (c).

In Figures 7(a) and (c), for the curves in Group 2, the growth velocities at the end are greater than those in Group 1. It seems that the boys/girls whose growth curves are in Group 2 continued to grow higher at great speed at age 18 and their growth velocity curves show a different pattern since the growth processes were not yet complete. With $\lambda_0 = 0.5$, we found that Group 1 contains growth curves of boys and girls, but Group 2 contains growth curves of only boys. Figures 7 (b) and (d) show the warping functions for $\lambda_0 = 0$ and 0.5. The warping functions for $\lambda_0 = 0.5$ are smoother than those for $\lambda_0 = 0$, as expected.

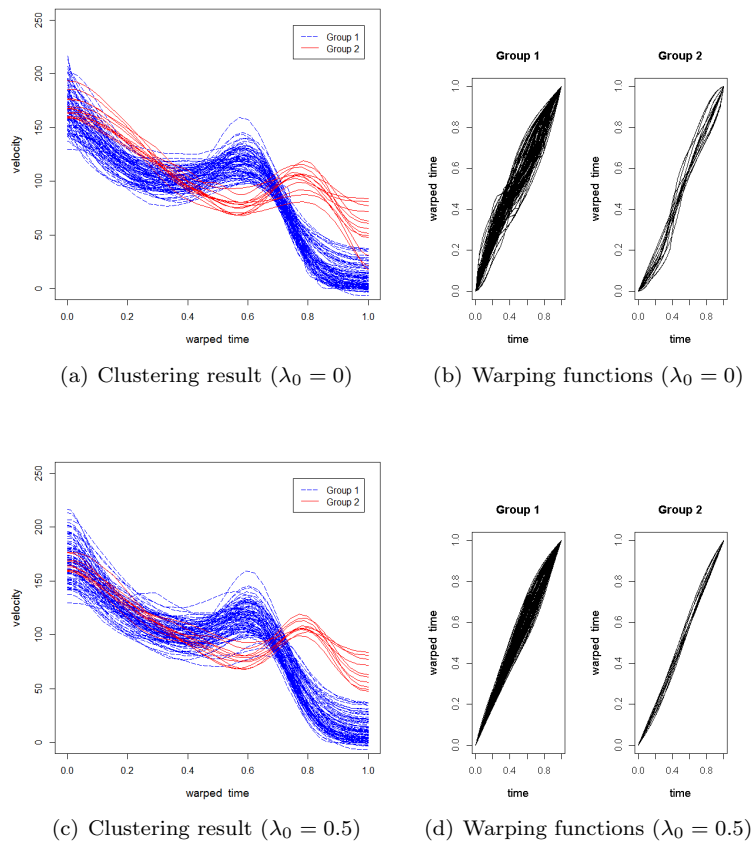


FIG 7. Clustering results and warping functions for growth study data

4.2. *Baby Finder data*

A Baby Finder is an electronic device comprising a receiver and a transmitter, where the transmitter can send signals to the receiver continuously. The Baby Finder data set contains signal loss data for a Baby Finder from eight trials, provided by the third author of this paper. For each trial, the transmitter and the receiver are put together first and then are taken away along two paths respectively. If the moving path pairs for two trials are the same, we expect the corresponding signal loss curves to be similar. Applying the proposed clus-

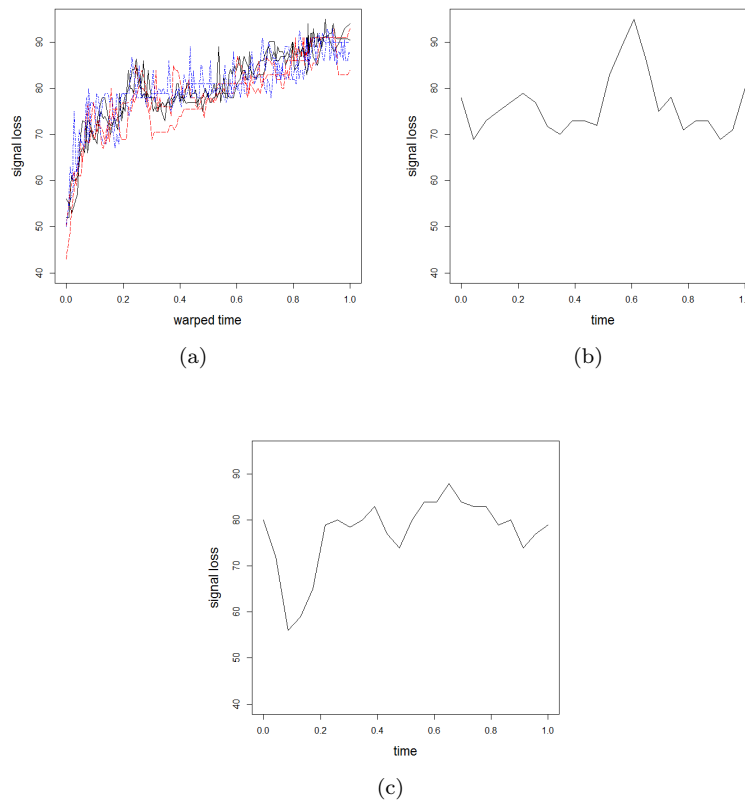


FIG 8. *Clustering results for Baby Finder data*

tering method to those signal loss curves, the eight curves are clustered into three groups. The curves in the three groups are shown in Figures 8(a)–(c), respectively. The left figure shows the aligned six curves for the first group, all of which increase as time increases. The rest two curves have different patterns corresponding to different moving paths, and thus the two are clustered into two singleton groups. For each of the six curves in the first group, in addition

to signal loss measurements, we have information on the travel distances of the receiver at different time points. We find that for the six trials, the signal losses at the same distance are about the same, and the maximum travel distances are the same, so we suspect that the receiver and the transmitter were taken away from the same pair of paths respectively for the six trials. The clustering results support our guess.

5. Discussion and suggestions

Based on our simulation results, the proposed method works well when warping functions satisfy the boundary condition. Regarding the implementation, one needs to choose S_c , the penalty parameter λ_0 and the clustering index. Below are our comments and suggestions when S_c is determined using q_{1-a} .

- When q_{1-a} is small, it takes very few iterations for the curves to be combined, but curves that are not very similar may be combined and may be put into the same cluster due to the small combination threshold values. As q_{1-a} increases, it can be ensured that only similar curves are combined but it takes more iterations for the curves to be combined. Based on our simulation experiments, the clustering results remain stable when q_{1-a} is between q_{45} and q_{85} . If q_{1-a} is too large, the curves may not be combined in the limited number of iterations and one may have to increase the limit for the number of iterations, and computation time can be longer. Our suggestion is to choose a large q_{1-a} (as large as possible, but not large enough to make the number of iterations reaches its limit).
- In most of our simulation experiments, we use $q_{1-a} = q_{75}$, and the computation takes a lot of time. For the case $(N1, N2, N3) = (10, 10, 10)$ and $\lambda_0 = 0$ in Table 1, the median computation times (three trials) for $\sigma = 0.45$ and $\sigma = 0.15$ are 22142 seconds and 7574 seconds respectively using a machine with Intel CPU i7-4790K. For the case where $(N1, N2, N3) = (10, 10, 20)$, $\lambda_0 = 0$, $\sigma = 0.15$, the median computation times (three trials) is 11133 seconds. If we use $q_{1-a} = q_{55}$, for the case where $(N1, N2, N3) = (10, 10, 10)$, $\lambda_0 = 0$, $\sigma = 0.15$, the median computation time (three trials) becomes 3970 seconds, which is much less than that of the case with $q_{1-a} = q_{75}$.
- The choice of λ_0 depends on to what extent time variation is considered as a clustering factor. Consider the case where one curve y_1 can be perfectly aligned to another curve y_2 using a warping function ψ , but ψ is very different from the identity function. In such case, if one would like y_1 and y_2 to be assigned into the same cluster (time variation is not important), then λ_0 should be set to 0. Otherwise, a nonzero λ_0 should be used. Using a large λ_0 means that time variation is considered as an important factor in clustering.
- Since the results based on the Dunn index are very similar to those based on the Silhouette index, the effect of clustering index does not seem to be significant. If one would like to choose a clustering index, it is rec-

ommended to use a clustering index that does not involve cluster centers (such as the Silhouette coefficient or the Dunn index) since the proposed method does not compute cluster centers in the clustering process.

6. Proofs

In the section, we give the proof of Theorem 1, and the proofs of two facts: Facts 1 and 2, which are used in the proof of Theorem 1. We will state and prove Facts 1 and 2 first.

We first state Fact 1. Let $V = L^2[0, 1]$. Below are the assumptions, statement and proof of Fact 1.

- (A1) Suppose that $h_1, \dots, h_k \in V$ and $g = \sum_{j=2}^k \theta_j h_j$, where θ_j s are constants in $[0, 1]$ such that $\sum_{j=2}^k \theta_j = 1$.
- (A2) Suppose that for $j = 2, \dots, k$, $\langle \cdot, \cdot \rangle_j$ is a positive semi definite symmetric bilinear form from $V \times V$ to R .
- (A3) For $j = 2, \dots, k$, let $\| \cdot \|_j$ be the semi-norm on V defined by $\|f\|_j = \sqrt{\langle f, f \rangle_j}$ for $f \in V$.
- (A4) Suppose that $\|h_j\|_j = 1$ for $j = 1, \dots, k$.
- (A5) Suppose that c_1, \dots, c_k are positive constants.

Fact 1. *Suppose that (A1)–(A5) hold. For $\lambda > 0$, let*

$$T(\lambda) = \sum_{j=2}^k \frac{c_j \langle \lambda h_1 + g, h_j \rangle_j}{\| \lambda h_1 + g \|_j}$$

and

$$T(\infty) = \lim_{\lambda \rightarrow \infty} T(\lambda) = \sum_{j=2}^k \frac{c_j \langle h_1, h_j \rangle_j}{\|h_1\|_j}.$$

Let $A_j = \frac{c_j \langle h_1, h_j \rangle_j}{\|h_1\|_j}$, $B_j = \frac{c_j \langle g, h_j \rangle_j}{\|h_1\|_j}$, $D_j = \frac{2 \langle h_1, g \rangle_j}{\|h_1\|_j^2}$, $E_j = \frac{\|g\|_j}{\|h_1\|_j}$, $\alpha_j = B_j - \frac{1}{2} A_j D_j$ and

$$\beta_j = \frac{1}{2} (A_j E_j^2 + B_j D_j + |B_j| E_j) + \frac{3}{\sqrt{2}} (|A_j| + 1) (|D_j| + E_j)^2.$$

If $\sum_{j=2}^k \alpha_j > 0$ and

$$\lambda \geq \max \left(\frac{\sum_{j=2}^k \beta_j}{\sum_{j=2}^k \alpha_j}, \max_{2 \leq j \leq k} \max(E_j, |B_j|) \right), \quad (9)$$

then $T(\lambda) \geq T(\infty)$.

Proof of Fact 1. Note that

$$T(\lambda) = \sum_{j=2}^k \frac{\lambda A_j + B_j}{\sqrt{\lambda^2 + \lambda D_j + E_j^2}} \text{ and } T(\infty) = \sum_{j=2}^k A_j.$$

Let $U_j = \frac{\lambda A_j + B_j}{\sqrt{\lambda^2 + \lambda D_j + E_j^2}} - A_j$, then $T(\lambda) - T(\infty) = \sum_{j=2}^k U_j$.

To find a lower bound for the expression

$$U_j = \frac{A_j + \frac{B_j}{\lambda}}{\sqrt{1 + \frac{D_j}{\lambda} + \frac{E_j^2}{\lambda^2}}} - A_j,$$

we consider the Taylor expansion of $1/\sqrt{1+x}$ at $x=0$, which gives

$$\frac{1}{\sqrt{1+x}} = 1 - \frac{1}{2}x + \frac{1}{2} \cdot \frac{3}{4}(1+c)^{-5/2}x^2,$$

where c is between 0 and x . Apply the result from Taylor expansion with $x = \frac{D_j}{\lambda} + \frac{E_j^2}{\lambda^2}$ and we have

$$\begin{aligned} U_j &= A_j \left(1 - \frac{1}{2} \left(\frac{D_j}{\lambda} + \frac{E_j^2}{\lambda^2} \right) + \frac{3\tilde{c}}{8} \left(\frac{D_j}{\lambda} + \frac{E_j^2}{\lambda^2} \right)^2 \right) \\ &\quad + \frac{B_j}{\lambda} \left(1 - \frac{1}{2} \left(\frac{D_j}{\lambda} + \frac{E_j^2}{\lambda^2} \right) + \frac{3\tilde{c}}{8} \left(\frac{D_j}{\lambda} + \frac{E_j^2}{\lambda^2} \right)^2 \right) \\ &\quad - A_j, \end{aligned} \tag{10}$$

where $\tilde{c} = (1+c)^{-5/2}$. Suppose that (9) holds, then $\lambda \geq E_j$, using the fact that $|D_j| \leq 2E_j$, we have

$$-\frac{1}{2} \leq \frac{D_j}{\lambda} + \frac{E_j^2}{\lambda^2} \leq 3,$$

which implies that $1+c \geq 0.5$ and $0 < \tilde{c} \leq 2^{5/2}$. It then follows from (9) and

(10) that

$$\begin{aligned}
U_j &\geq \frac{1}{\lambda} \left(B_j - \frac{1}{2} A_j D_j \right) \\
&\quad - \frac{1}{2} \frac{A_j E_j^2}{\lambda^2} - \frac{3\tilde{c}}{8} |A_j| \left(\frac{|D_j| + E_j}{\lambda} \right)^2 \\
&\quad - \frac{1}{2\lambda^2} (B_j D_j + |B_j| E_j) - \frac{3\tilde{c}}{8} \frac{|B_j| (|D_j| + E_j)^2}{\lambda^2} \\
&\geq \frac{1}{\lambda} \left(B_j - \frac{1}{2} A_j D_j \right) \\
&\quad - \frac{1}{\lambda^2} \left(\frac{1}{2} (A_j E_j^2 + B_j D_j + |B_j| E_j) \right) \\
&\quad - \frac{1}{\lambda^2} \left(\frac{3(2^{5/2})}{8} (|A_j| + 1) (|D_j| + E_j)^2 \right) \\
&= \frac{\alpha_j}{\lambda} - \frac{\beta_j}{\lambda^2}.
\end{aligned}$$

Thus for $\lambda \geq \sum_{j=2}^k \beta_j / \sum_{j=2}^k \alpha_j$, $\sum_{j=2}^k U_j \geq 0$. Therefore, $T(\lambda) - T(\infty) = \sum_{j=2}^k U_j \geq 0$ when (9) holds. The proof of Fact 1 is complete.

Next, we give the assumptions, statement and proof of Fact 2.

(A6) Suppose that $\langle \cdot, \cdot \rangle$ is a positive semi definite symmetric bilinear form from $V \times V$ to R .

(A7) Let $\| \cdot \|$ be the semi-norm on V defined by $\|f\| = \sqrt{\langle f, f \rangle}$ for $f \in V$.

(A8) Suppose that $\|h_j\| = 1$ for $j = 1, \dots, k$.

Fact 2. Suppose that (A1) and (A6)–(A8) holds. Let $s = \sum_{j=2}^k h_j$. For $\lambda > 0$, let

$$T(\lambda) = \sum_{j=2}^k \frac{\langle \lambda h_1 + g, h_j \rangle}{\| \lambda h_1 + g \|} = \frac{\langle \lambda h_1 + g, s \rangle}{\| \lambda h_1 + g \|}$$

and

$$T(\infty) = \lim_{\lambda \rightarrow \infty} T(\lambda) = \sum_{j=2}^k \frac{\langle h_1, h_j \rangle}{\|h_1\|} = \sum_{j=2}^k \langle h_1, h_j \rangle = \langle h_1, s \rangle.$$

Let

$$r(g) = g - \langle g, h_1 \rangle h_1$$

and

$$r(s) = s - \langle s, h_1 \rangle h_1.$$

If $\langle h_j, h_1 \rangle \geq 0$ for every $j \geq 2$, $\langle r(g), r(s) \rangle > 0$, $\lambda > 0$ and

$$\lambda \geq \frac{\|r(g)\|^2 \langle s, h_1 \rangle^2 - \langle r(g), r(s) \rangle^2}{2 \langle s, h_1 \rangle \langle r(g), r(s) \rangle} - \langle g, h_1 \rangle, \quad (11)$$

then $T(\lambda) \geq T(\infty)$.

Proof of Fact 2. Let $\beta = \lambda + \langle g, h_1 \rangle$, then

$$\begin{aligned} T(\lambda) - T(\infty) &= \frac{\beta \langle h_1, s \rangle + \langle r(g), r(s) \rangle}{\sqrt{\beta^2 + \|r(g)\|^2}} - \langle s, h_1 \rangle \\ &= \left(\frac{\beta \langle h_1, s \rangle + \langle r(g), r(s) \rangle}{\sqrt{\beta^2 + \|r(g)\|^2}} \right)^2 - \langle s, h_1 \rangle^2 \\ &= \frac{\frac{\beta \langle h_1, s \rangle + \langle r(g), r(s) \rangle}{\sqrt{\beta^2 + \|r(g)\|^2}} + \langle s, h_1 \rangle}{\sqrt{\beta^2 + \|r(g)\|^2}}. \end{aligned}$$

Under the conditions that $\lambda > 0$, $\langle h_j, h_1 \rangle \geq 0$ for every $j \geq 2$ and $\langle r(g), r(s) \rangle > 0$, we have $\langle s, h_1 \rangle \geq \|h_1\|^2 = 1$ and

$$\frac{\beta \langle h_1, s \rangle + \langle r(g), r(s) \rangle}{\sqrt{\beta^2 + \|r(g)\|^2}} + \langle s, h_1 \rangle > 0,$$

so

$$\begin{aligned} T(\lambda) &\geq T(\infty) \\ &\Leftrightarrow (\beta \langle h_1, s \rangle + \langle r(g), r(s) \rangle)^2 - (\beta^2 + \|r(g)\|^2) \langle s, h_1 \rangle^2 \geq 0 \\ &\Leftrightarrow 2\beta \langle s, h_1 \rangle \langle r(g), r(s) \rangle \geq -\langle r(g), r(s) \rangle^2 + \|r(g)\|^2 \langle s, h_1 \rangle^2 \\ &\Leftrightarrow (11) \text{ holds.} \end{aligned}$$

The proof of Fact 2 is complete.

Next, we provide the proof of Theorem 1 as follows.

Proof of Theorem 1. To establish

$$\sum_{j=2}^k \rho(f_1, f_j) \leq \sum_{j=2}^k \rho(\lambda f_1 + g_0, f_j) = \sum_{j=2}^k \rho(f_1^*, f_j), \quad (12)$$

we will prove

$$\sum_{j=2}^k r(f_1, f_j \circ \psi_j) \leq \sum_{j=2}^k r(\lambda f_1 + g_0, f_j \circ \psi_j) \quad (13)$$

and

$$\sum_{j=2}^k r(f_1 \circ \psi_j^{-1}, f_j) \leq \sum_{j=2}^k r((\lambda f_1 + g_0) \circ \psi_j^{-1}, f_j). \quad (14)$$

Then

$$\begin{aligned}
\sum_{j=2}^k \rho(f_1, f_j) &= \sum_{j=2}^k \rho(f_1, f_j | \psi_j) \\
&= \sum_{j=2}^k \frac{1}{2} \left(r(f_1, f_j \circ \psi_j) - \lambda_0 \int_0^1 \left(\frac{d}{dt} \psi_j(t) - 1 \right)^2 dt \right) \\
&\quad + \sum_{j=2}^k \frac{1}{2} \left(r(f_1 \circ \psi_j^{-1}, f_j) - \lambda_0 \int_0^1 \left(\frac{d}{dt} \psi_j^{-1}(t) - 1 \right)^2 dt \right) \\
&\stackrel{(13),(14)}{\leq} \sum_{j=2}^k \rho(\lambda f_1 + g_0, f_j | \psi_j) \\
&\leq \sum_{j=2}^k \rho(\lambda f_1 + g_0, f_j)
\end{aligned}$$

and (12) holds.

To prove (13), note that (13) follows from Fact 2 with $h_1 = f_1$, $g = g_0$ and $h_j = \frac{f_j \circ \psi_j}{\|f_j \circ \psi_j\|}$ for $j \geq 2$. The required conditions are implied by (C1)–(C3) and (C5).

To prove (14), we will apply Fact 1. For $f \in V$,

$$r(f \circ \psi_j^{-1}, f_j) = \frac{\langle f, f_j \circ \psi_j \rangle_j}{\|f\|_j}.$$

Apply Fact 1 with $h_1 = f_1$, $c_j = \|f_j \circ \psi_j\|$ and $h_j = f_j \circ \psi_j / c_j$ for $j \geq 2$. Then (14) holds if $\sum_{j=2}^k \alpha_j > 0$ and (9) holds. Note that $\sum_{j=2}^k \alpha_j > 0$ is equivalent to the condition (C4) and (9) is given in (C6). Therefore, (14) holds.

References

- T.-L. Chen and S.-Y. Shiu. A new clustering algorithm based on self-updating process. In *Proceedings of the American Statistical Association, Statistical Computing Section [CD-ROM]*, Salt Lake City, Utah. (2007).
- J. C. Dunn. Well separated clusters and optimal fuzzy partitions. *Journal of Cybernetics*, 4:95–104 (1974).
- K. Fukunaga and L. D. Hostetler. The estimation of the gradient of a density function, with applications in pattern recognition. *IEEE Transactions on Information Theory*, 21:32–40 (1975).
- D. Gervini and T. Gasser. Self-modelling warping functions. *Journal of the Royal Statistical Society, Series B: Statistical Methodology*, 66:959–971 (2004).
- L. Hubert and P. Arabie. Comparing partitions. *Journal of Classification*, 2: 193–218 (1985).
- J. Jacques and C. Preda. Functional data clustering: a survey. *Advances in Data Analysis and Classification*, 8:231–255 (2014).

- G. M. James. Curve alignment by moments. *The Annals of Applied Statistics*, 1:480–501 (2007).
- A. Kneip and T. Gasser. Statistical tools to analyze data representing a sample of curves. *The Annals of Statistics*, 20:1266–1305 (1992).
- A. Kneip, X. Li, K. B. MacGibbon, and J. O. Ramsay. Curve registration by local regression. *The Canadian Journal of Statistics/La Revue Canadienne de Statistique*, 28:19–29 (2000).
- X. Liu and M. C. Yang. Simultaneous curve registration and clustering for functional data. *Computational Statistics & Data Analysis*, 53:1361–1376 (2009).
- J. O. Ramsay and X. Li. Curve registration. *Journal of the Royal Statistical Society, Series B: Statistical Methodology*, 60:351–363 (1998).
- J. O. Ramsay and B. W. Silverman. *Functional Data Analysis*. Springer-Verlag Inc (1997). ISBN 0-387-94956-9.
- P. J. Rousseeuw. Silhouettes: A graphical aid to the interpretation and validation of cluster analysis. *Journal of Computational and Applied Mathematics*, 20:53 – 65 (1987).
- L. M. Sangalli, P. Secchi, S. Vantini, and V. Vitelli. k -mean alignment for curve clustering. *Computational Statistics & Data Analysis*, 54:1219–1233 (2010).
- S.-Y. Shiu and T.-L. Chen. Clustering by self-updating process. In *arxiv:1201.1979* (2012).
- B. W. Silverman. Incorporating parametric effects into functional principal components analysis. *Journal of the Royal Statistical Society, Series B: Methodological*, 57:673–689 (1995).
- J. Soler, F. Tencé, L. Gaubert, and C. Buche. Data clustering and similarity. In *Proceedings of the Twenty-Sixth International Florida Artificial Intelligence Research Society Conference*, pages 492–495, St. Pete Beach, Florida. (2013).
- R. Tang and H.-G. Müller. Time-synchronized clustering of gene expression trajectories. *Biostatistics*, 10:32–45 (2009).
- D. Telesca and L. Y. T. Inoue. Bayesian hierarchical curve registration. *Journal of the American Statistical Association*, 103:328–339 (2008).
- R. D. Tuddenham and M. M. Snyder. Physical growth of california boys and girls from birth to eighteen years. In *University of California Publications in Child Development*, volume 1, pages 183–364. University of California Press (1954).
- S. Zhou and X. Shen. Spatially adaptive regression splines and accurate knot selection schemes. *Journal of the American Statistical Association*, 96:247–259 (2001).